Kinetics of NCl($a^1\Delta$ and $b^1\Sigma^+$) Generation: The Cl + N_3 Rate Constant, the NCl($a^1\Delta$) Product Branching Fraction, and Quenching of NCl($a^1\Delta$) by F and Cl Atoms

G. C. Manke II and D. W. Setser*

Department of Chemistry, Kansas State University, Manhattan, Kansas 66506

Received: March 24, 1998; In Final Form: July 7, 1998

The quenching rate constants for NCl($a^1\Delta$) by F and Cl atoms have been measured at room temperature to be $(2.2 \pm 0.7) \times 10^{-11}$ and $(1.0 + 1.0/-0.5) \times 10^{-12}$ cm^3 s^{-1}, respectively, by adding F and Cl atoms to a flow reactor containing NCl($a^1\Delta$). With knowledge of these quenching rate constants, the kinetics for the formation of NCl($a^1\Delta$) from the Cl + N_3 reaction could be investigated in the F/Cl/HN_3 reaction system. The reduction in NF($a^1\Delta$) yield from adding Cl atoms to the reactor containing F and HN_3 and the relative NF($a^1\Delta$) and NCl($a^1\Delta$) yields for known concentrations of F and Cl atoms in this reaction system favor a total Cl + N_3 rate constant of $3 \pm 1 \times 10^{-11}$ cm^3 s^{-1} with a branching fraction for NCl($a^1\Delta$) formation of $\gtrsim$ 0.5. The branching fraction was deduced from comparing the relative intensities of the NCl(a−X) and NF(a−X) transitions using a lower limit to the NCl(a) radiative lifetime of 2 s. The direct formation of NCl($b^1\Sigma^+$) from Cl + N_3 is a minor channel; however, NCl($b^1\Sigma^+$) is formed by bimolecular energy pooling of NCl($a^1\Delta$) molecules with a rate constant of $\approx 1.5 \times 10^{-13}$ cm^3 s^{-1} and by energy transfer between NCl($a^1\Delta$) and HF($v \geq 2$). The bimolecular energy-pooling process is a small fraction of the total bimolecular self-destruction rate for NCl($a^1\Delta$).

I. Introduction

The reactions of H atoms with NF_2 and F atoms with N_3 are excellent gas phase sources of NF($a^1\Delta$).[1−8] In each case the ground singlet state molecule is formed, HNF_2 or FN_3, that subsequently undergoes unimolecular decomposition before collisional stabilization at modest pressures. Since spin is conserved, NF($a^1\Delta$) is formed rather than NF($X^3\Sigma^-$). Both systems have been thoroughly studied, and the efficiencies for NF($a^1\Delta$) formation are established[3−5] as ≥0.9 for H + NF_2 and ≥0.85 for F + N_3. The N_3 radical is generated by the reaction of F with HN_3.[5,7] Recent work has shown that the F + HN_3 reaction also gives $3 \pm 2\%$ HNF + N_2 at room temperature.[9,10] However, HNF probably reacts with excess F atoms to give vibrationally excited HNF_2*, which also decomposes to NF($a^1\Delta$) at <10 Torr pressure. Fortunately, the H and F + NF($a^1\Delta$) reactions have small rate constants, (3.1 ± 0.6) and $(4.0 \pm 2.0) \times 10^{-13}$ cm^3 molecule^{-1} s^{-1}, respectively,[11,5b] at 300 K, and excess concentrations of H and F atoms can be used to obtain high concentrations of NF($a^1\Delta$). A less satisfactory characteristic of NF($a^1\Delta$) for energy storage applications is the bimolecular self-destruction process,[5b] which has a rate constant (defined by $-d[NF(a)]/dt = k_{bi}[NF(a)]^2$) of $(5 \pm 2) \times 10^{-12}$ cm^3 molecules^{-1} s^{-1}. The reaction of Cl atoms with N_3 offers an attractive possibility for a source of NCl($a^1\Delta$) molecules. The reaction rate of Cl atoms with HN_3 at 300 K is too slow to be a useful source of N_3 in a flow reactor,[12,13] and most investigators have added F atoms to the Cl/HN_3 system to achieve higher concentrations of NCl($b^1\Sigma^+$) or NCl($a^1\Delta$), although the simultaneous presence of F and Cl atoms adds chemical complexity to the system.[14,15] The main goal of the present work was to assign the total rate constant and the branching fractions, X_a, X_b, and X_x for the product channels in reaction 1 as part of our effort to characterize the F/Cl/HN_3 reaction system as a chemical source of NCl($a^1\Delta$).

$$Cl(^2P) + N_3(X^2\Pi) \rightarrow ClN_3^* \rightarrow NCl(a^1\Delta) + N_2 \quad (1a)$$

$$\rightarrow NCl(b^1\Sigma^+) + N_2 \quad (1b)$$

$$\rightarrow NCl(X^3\Sigma^-) + N_2 \quad (1c)$$

The $\Delta H°$ values for eqs 1a−1c are −39, −22, and −65 kcal mol^{-1}, respectively, for $\Delta H_f°(N_3)$[5a,16] = 113.6 and $\Delta H_f°(NCl)$[17] = 77.4 kcal mol^{-1}. All experiments were done in a flow reactor at room temperature.

In order to measure X_a and the rate constant for reaction 1, the NCl($a^1\Delta$) removal processes must be understood. In particular, the quenching rates by F and Cl atoms are required. The NCl(a) bimolecular self-destruction and the bimolecular NF($a^1\Delta$) + NCl($a^1\Delta$) rates are not important if concentrations below $\sim 2 \times 10^{12}$ molecule cm^{-3} are used. The competition between F and Cl atoms reacting with N_3 already has been reported;[8] however, our experiments, similar work by Henshaw and co-workers,[18a] and a direct measurement using laser-induced fluorescence to monitor the decay of [N_3] with added [Cl][19] support a k_1 value that is slightly smaller than the F + N_3 rate constant ($(5 \pm 2) \times 10^{-11}$ cm^3 s^{-1})[6,7] rather than eight times larger.[7] Our value for k_1 is based upon the reduction in NF(a) concentration as Cl atoms are added to the system and on the time dependence for the generation of NF(a) and NCl(a). Our strategy for obtaining the branching fractions for reaction 1 is to measure the relative concentrations of NCl($a^1\Delta$) and NF($a^1\Delta$) for known initial F, Cl, and HN_3 concentrations in the flow reactor. In the absence of Cl atoms, excess [F] will convert the [HN_3] to a known [NF(a)], and the emission intensity from [NCl(a)] can be compared to the emission intensity from the known [NF(a)]. These relative concentrations are obtained from the relative a−X emission intensities at 874 and 1077 nm from NF(a) and NCl(a), respectively, with a monochromator fitted with an S-1 response photomultiplier tube. Since the lifetimes

S1089-5639(98)01603-X CCC: $15.00
Published on Web 08/19/1998

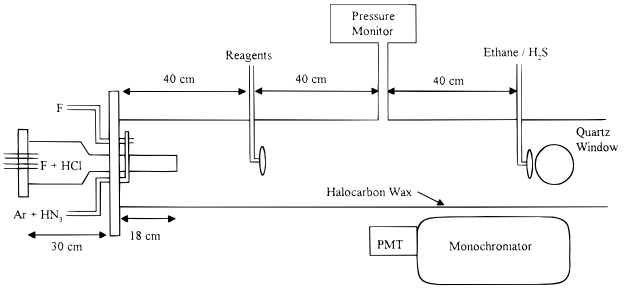

Figure 1. Schematic diagram of the Pyrex glass flow-reactor. The inner pre-reactor was used to produce Cl atoms from the F + HCl reaction. The fore-reactor was used as an independent F-atom source. The HN_3 could be added to the fore-reactor or at the reagent position. The C_2H_6 or H_2S were added near the end of the reactor for monitoring the F- and Cl-atom concentrations. The diameter of the main reactor was 7.0 cm; the pre-reactor section was constructed from 4.0 and 3.0 cm diameter tubing.

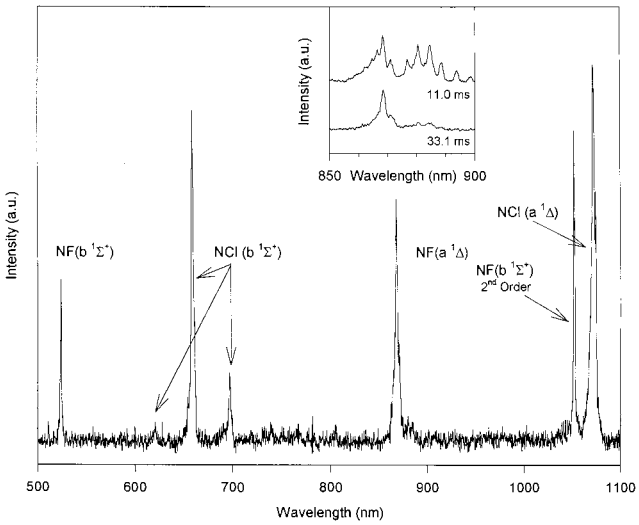

Figure 2. Representative spectra from the F/Cl/HN_3 reaction system after a reaction time of 30 ms. The inset shows the HF(3−0) and NF(a−X) emissions at higher resolution. The HF(3−0) emission was insignificant 30 ms downstream of the HN_3 inlet. A cut-off filter normally was placed in front of the slit of the monochromator to eliminate the second-order spectra. Spectra acquired in the Cl + N_3 reaction zone showed only the 0−0 band of the NCl(a−X) emission and reaction 1a gives virtually no $v' = 1$ product.

of NF(a) and NCl(a) are very long, the emission intensities must be related to concentrations by Einstein coefficients, $I(\mathrm{NCl(a)}) = \tau^{-1}_{\mathrm{NCl}}[\mathrm{NCl(a)}]$ and $I(\mathrm{NF(a)}) = \tau^{-1}_{\mathrm{NF}}[\mathrm{NF(a)}]$. The NF($a^1\Delta$) lifetime is accepted[4c,6] as 5 s. The best calculated lifetime[20] for NCl($a^1\Delta$) is 2.4 s. The decay time for NCl(a) in a matrix isolation experiment[21] can be adjusted to an equivalent gas-phase value of 3.7 s. We have selected a lower limit of $\tau_{\mathrm{NCl(a)}} = 2$ s for our calculations, which leads to a lower limit for X_a. Other investigators have made a similar choice.[18]

Before the data needed to obtain the branching fraction for NCl(a) formation are presented, the decay kinetics of NF(a) and NCl(a) as a function of the F- and Cl-atom concentrations is examined in order to assign these quenching rate constants. The NCl(a) bimolecular self-destruction rate constant[18b] is reported to be $5-8 \times 10^{-12}$ cm^{-1} s^{-1}, which is of similar magnitude as for NF(a).[5b] We worked at sufficiently low [NCl(a)] concentrations such that this bimolecular loss process is not very important. A few experiments also were done with the Cl + HN_3 reaction system in order to assign the rate constant for bimolecular energy pooling from 2NCl(a), to confirm the X_a result obtained in the F/Cl/HN_3 system and to find an upper limit to X_b.

II. Experimental Methods

Most experiments were performed in the flow reactor shown in Figure 1. The inner pre-reactor was designed to generate Cl atoms by the relatively slow F + HCl reaction ($k = 0.94 \times 10^{-11}$ cm^3 s^{-1}).[22] The Ar carrier gas was purified by passage through cooled (−77 °C for high pressure and −196 °C for low pressure) molecular sieve filled traps. The maximum flow velocity in the main reactor provided by a small Roots blower plus mechanical pump was 12 m s^{-1}. This could be reduced by partly closing a gate valve, and velocities of 3.5 m s^{-1} were commonly used. The reactor walls plus the inner and outer walls of the pre-reactor were coated with halocarbon wax to reduce the loss of F and Cl atoms and N_3 radicals on the surfaces of the reactor. Fluorine atoms were generated in both the fore-reactor and pre-reactor by a microwave discharge through dilute flows of CF_4 in Ar. Unit efficiency for the generation of Cl atoms by the F + HCl reaction was confirmed by measuring the Cl-atom concentration. Thus, loss of Cl atoms in the pre-reactor was not significant. The HN_3 could be added to the reactor either at the entrance to the fore-reactor or at the reagent port on the main reactor. The Ar and CF_4 flow rates were measured by Hastings mass flow meters. The flow rates of HN_3, HCl, and all other reagents were measured by observing the pressure rise in a bulb of known volume. The HN_3 was prepared by heating sodium azide with stearic acid; it was stored as a 10% mixture in Ar in a 12 L reservoir. The purity was confirmed by mass spectrometric analysis. The CF_4 and HCl were obtained from commercial suppliers.

The relative Cl-atom concentrations were monitored by the relative intensities of the HCl($\Delta v = -1$) transition at 2900 cm^{-1} using an InSb infrared detector with an interference filter; the HCl($v \leq 1, 2$) molecules were generated by the Cl + H_2S reaction. The [F] was measured by monitoring the HF($\Delta v = -3$) relative intensity at 850 nm with the monochromator and photomultiplier tube; the HF was produced by the addition of H_2S or C_2H_6 near the end of the reactor. The absolute F and Cl atom concentrations were calibrated by titration with CF_3I and C_2H_3Br, respectively. These titration reactions for F and Cl atoms have been described in separate publications.[5,13]

Emission spectra from NF($a^1\Delta$), NF($b^1\Sigma^+$), NCl($a^1\Delta$), NCl($b^1\Sigma^+$), and HF(3−0) transitions were observed with a 0.5 m Minuteman monochromator equipped with a grating blazed at 1000 nm with 600 lines mm^{-1}; see Figure 2. The slits were usually set to 1 mm, which corresponds to a resolution of 3.3 nm. The monochromator was mounted on a moveable table so that the emission could be monitored along the length of the flow tube. A S-1 type photomultiplier tube (PMT), Hammamatsu R1767 selected for enhanced red sensitivity, was used to observe the NCl($a^1\Delta - X^3\Sigma^-$) transition at 1077 nm. The dark current at room temperature and 1250 V, typically 7000 nA, was reduced by a liquid-nitrogen cooled housing (Products for Research, model TE176TSRF). The temperature, which was adjustable from 20 to −110 °C, normally was −80 °C, and the dark current was 10−15 pA. The current from the PMT was monitored by a Keithley electrometer (model 614) and recorded on a 386 personal computer using a Keithley data acquisition card (model DAS-8). The response of the detection system vs wavelength was calibrated using a standard quartz-iodine lamp.

The relative [NF(a)] and [NCl(a)] were obtained by multiplying the observed NF(a−X) and NCl(a−X) intensities by the appropriate conversion factor, which is the product of the respective Einstein coefficients (or the inverse of the radiative

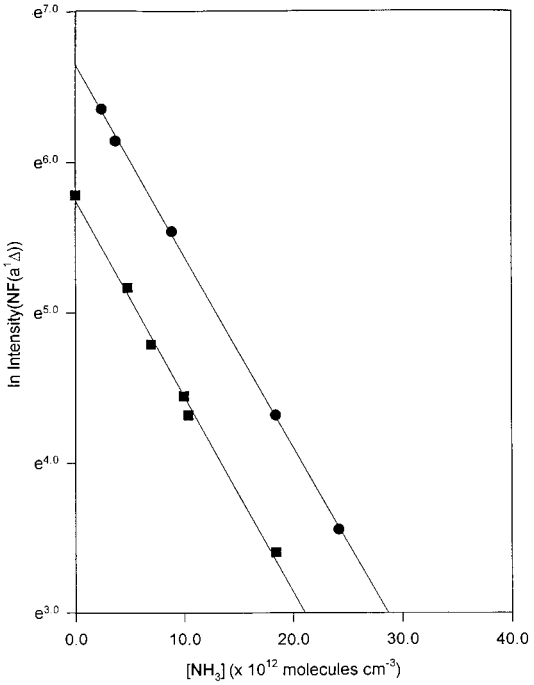

Figure 3. Pseudo-first-order quenching plots of NF(a) by NH_3 with (□) and without (●) added Cl atoms. The I(NF(a)) was measured 80 cm from the reagent inlet, and the initial concentrations were $[HN_3] = 1.7 \times 10^{12}$, $[F] = 1.5 \times 10^{12}$, and $[Cl] = 1.1 \times 10^{12}$ cm^{-3}. For $k_{NH_3}^{NF} = 3.6 \times 10^{-12}$ cm^3 s^{-1} the reaction time, Δt, is 0.037 s.

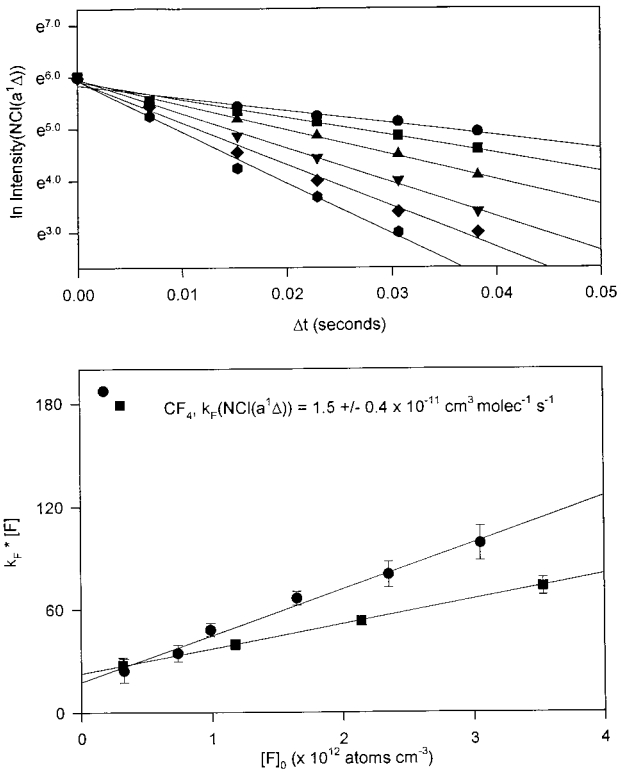

Figure 4. Pseudo-first-order decay plots of NCl(a) vs time for a range of F-atom concentration generated from CF_4. The lower panel shows a plot of the slopes, $k_F[F]$, from the top panel vs [F], plus the same information from a second similar experiment.

lifetime), the relative sensitivity of the detector, and the respective spectral band areas. Both reactions give mainly $v' = 0$ molecules and only the 0−0 bands need to be considered. The ratio of response at 874 vs 1077 nm was 2.1, and the transitions had the same bandwidths for a 1 mm slit. For 5 and 2 s lifetimes, the I(NF(a))/I(NCl(a)) ratio was converted to the [NF(a)]/[NCl(a)] ratio by multiplying by a factor of 1.2.

An InSb infrared detector (Infrared Associates, $D^* = 2.16 \times 10^{11}$ cm Hz$^{0.5}$ W^{-1}) was used to measure HCl(1-0) intensity for Cl atom titrations.[13] The background thermal radiation was reduced, and the HCl emission was isolated by a band-pass filter (Perkin Elmer). A mechanical light-chopper was placed in front of the detector, and the signal was processed by a home-made preamplifier and a lock-in amplifier.

III. Experimental Results

III.A. Quenching Rate Constants of NCl(a) and NF(a) by Cl and F Atoms. Both fixed- and moving-point detection methods were used to measure the NF(a) and NCl(a) quenching rate constant under pseudo-first-order kinetic conditions. Although all flow calibrations were made and plug flow should have been established in the reactor, an empirical calibration of the reaction time, Δt, following addition of a reagent was made using the established rate constant for quenching of NF(a) by NH_3.[5b] The NF(a) concentration was generated from the F + HN_3 reaction in the fore-reactor, and NH_3 was added at the reagent inlet. For pseudo first-order kinetics with fixed-point detection, a plot of ln I(NF(a)) vs [reagent] has a slope equal to the product, $k_Q\Delta t$. The results for quenching of NF(a) with (1.1×10^{12} atoms cm^{-3}) and without the presence of Cl atoms are shown in Figure 3. The Cl atoms were generated by a second discharge through CF_2Cl_2 and added through the pre-reactor. Both plots have the same slope, and using $k_{NH_3}^{NF} = (3.6 \pm 0.2) \times 10^{-12}$ cm^3 s^{-1} gives an effective Δt of 0.037 s. The plug-flow prediction of Δt using the full distance between the reagent inlet and the observation point is 0.044 s. In addition to establishing the effective reaction time, these data demonstrate that the flow reactor was functioning as expected[5,6] for the F + HN_3 reaction system. Furthermore, nothing unusual occurs with respect to quenching of NF(a) by NH_3 if Cl atoms are introduced into the reactor for concentrations $\leq 1 \times 10^{13}$ cm^{-3} after the 2F + HN_3 reaction was complete, as shown in Figure 3, or in the fore-reactor zone (using the method described in the paragraph below). The HF(3−0) emission generated from F + HN_3 was observable for only the first 10 cm in the fore-reactor for the F and HN_3 concentrations and times used here. The F + NH_3 reaction mainly gives HF($v \leq 2$), and excess F atoms in the reactor does not interfere with the NF(a−X) emission used for monitoring the quenching of NF(a) by NH_3.

In order to study quenching of NCl(a) by F atoms, the F + HCl pre-reactor shown in Figure 1 was replaced by a simple discharge tube through which CF_2Cl_2 was passed to generate Cl atoms that subsequently reacted with N_3 to produce NCl(a). The concentrations in the fore-reactor were adjusted so that [NCl(a)] and [NF(a)] were nearly constant along the main reactor in the absence of excess F atoms (added as a quenching reagent). An additional flow of F atoms was added at the reagent inlet using a third microwave discharge through a flow of CF_4 or SF_6. The absolute [F] was determined by titration with CF_3I in the usual way.[5] For a given concentration of F atoms, the NCl(a) emission intensity was measured along the reactor, and plots of ln I(NCl(a)) vs time are linear with a slope equal to k_F^{NCl}[F]. The quenching rate constant was obtained by plotting the slopes of the pseudo-first-order quenching plots vs [F]. Figures 4 and 5 show representative data, and the rate constants and the conditions for these and other experiments are summarized in Table 1.

The rate constants from the four experiments in Table 1 vary between 2.87 and 1.51×10^{-11} cm^3 s^{-1}, and we conclude that

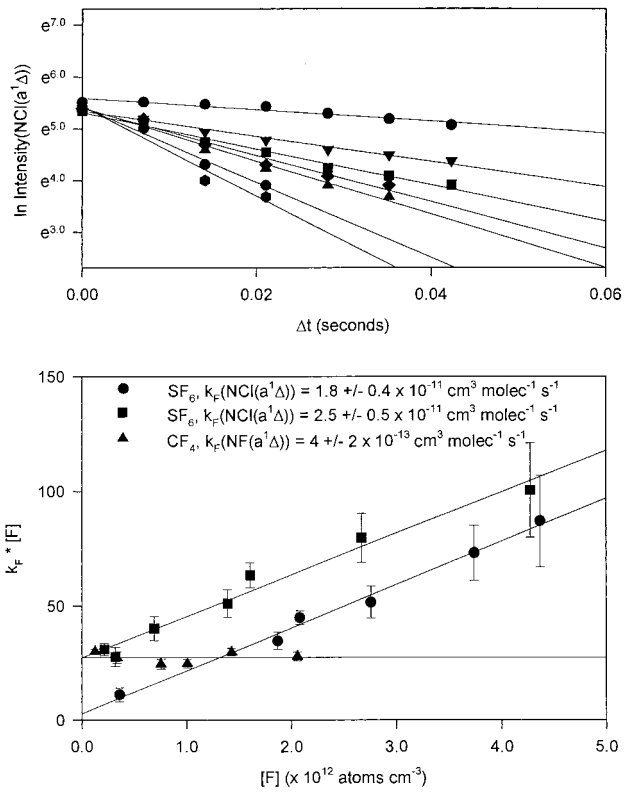

Figure 5. Pseudo-first-order decay plot of NCl(a) vs time for a range of F-atom concentration generated from SF_6. The lower panel shows the slopes of the decay plots vs [F]. Data from an experiment with NF(a) illustrating the absence of quenching also is shown for comparison. The K_F^{NF} value is from the literature.[5b]

TABLE 1: Quenching of NCl(a$^1\Delta$) by F Atoms

Cl/F source	$[Cl]_0$[a]	$[F]_0$[a]	$[HN_3]_0$[a]	$[F]_{added}$[b]	k_F^{NCl} [c]
CF_2Cl_2/CF_4	6.0	4.7	3.3	0−3.0	2.87 ± 0.43
$CFCl_3/CF_4$	2.7	4.2	1.9	0−5.8	1.51 ± 0.41
$CFCl_3/SF_6$	2.7	4.2	1.9	0−4.8	1.81 ± 0.43
$CFCl_3/SF_6$	5.2	2.4	1.2	0−4.4	2.52 ± 0.52

[a] The starting concentrations in the fore-reactor in units of 10^{12} molecules cm^{-3}. The $[Cl]_0$ was estimated from the fractional dissociation of CF_2Cl_2. [b] The range of [F] in units of 10^{12} molecules cm^{-3} added as a reagent using the F-atom source specified in column 1. [c] In units of 10^{-11} cm^3 molecule^{-1} s^{-1}.

$k_F^{NCl} = (2.2 \pm 0.7) \times 10^{-11}$ cm^3 s^{-1}. The F + NCl(a) rate constant is more than an order of magnitude larger than for F + NF(a),[5b,6c] which is $(4.0 \pm 2.0) \times 10^{-13}$ cm^3 s^{-1}. The plot in Figure 5 confirms this difference by showing that NF(a$^1\Delta$) was not quenched over the [F] range that gives nearly complete removal of NCl(a). No difference in k_F^{NCl} was noted for CF_4 or SF_6 as the F atom source. The possibility that the quenching of NCl(a) was a consequence of the presence of species from the discharge, such as CF_2, CF_3 or SF_5, rather than F atoms, was checked by doing some experiments using a discharge through F_2 as the F atom source.[23] Those experiments also gave a similar value for the k_F^{NCl} rate constant. The large value for k_F^{NCl} is consistent with our general observation that NCl(a) was always quenched whenever the [F] was high, regardless of whether F was added at the reagent port, the fore-reactor, or the pre-reactor.

The data shown in Figures 4 and 5 appear to follow pseudo-first-order kinetics to within the experimental uncertainty. However, for the low F atom concentration range, [F] ≈ [NCl(a)] and pseudo-first-order conditions do not actually apply unless [F] is constant, i.e., unless quenching occurs by physical energy transfer rather than by chemical reaction (formation of NF(a) + Cl is 4 kcal mol^{-1} exoergic). In an attempt to distinguish between chemical and physical quenching, an experiment with [F] ≈ [NCl(a)] was performed.[23b] If the chemical reaction converts F atoms to NF(a or X), the decay of [NCl(a)] should be described by the bimolecular rate law. Although the data seemed to fit first-order decay better than second-order decay, the [NCl(a)] range was too small to be certain. The simultaneously measured NF(a) emission intensity did not systematically increase as NCl(a) was removed. We conclude that quenching of NCl(a) occurs mainly by physical quenching and/or by formation of NF(X) + Cl.

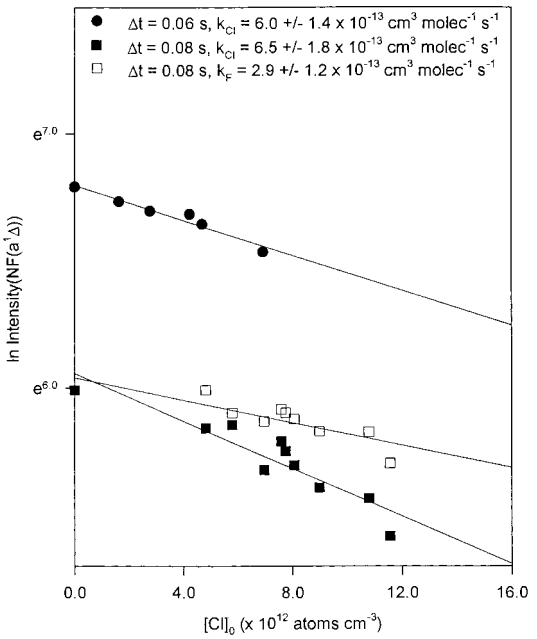

Figure 6. Pseudo-first-order quenching plots of NF(a) by [Cl] for fixed observation time of 0.06 or 0.08 s. The Cl atoms were generated in the pre-reactor by the F + HCl reaction. An experiment, □, also is shown for quenching NF(a) by F atoms for comparison. The latter was obtained by stopping the HCl flow to the pre-reactor.

The quenching of NCl(a) and NF(a) by Cl atoms was studied using the reactor shown in Figure 1; the F- and Cl-atom concentrations were measured by titration. Since a microwave discharge in CF_2Cl_2 gives both F and Cl atoms (in a 1/14 ratio)[13] and since the discharge through $CFCl_3$ may generate other species (such as Cl_2, CCl_2, or CCl) that quench NF(a) at the required high flows of $CFCl_3$, we used the F + HCl reaction under throttled conditions to study quenching of NF(a) by Cl atoms. The fore-reactor conditions were chosen so that $[F]_0 \approx 2[HN_3]_0$. The Cl + NF(a) quenching measurements are straightforward, since the F + HCl pre-reactor conditions can be controlled to provide the requisite [Cl]. The two experiments shown in Figure 6 are in agreement and give a rate constant of $(6 \pm 2) \times 10^{-13}$ cm^3 s^{-1}. A direct comparison of F and Cl + NF(a) quenching was accomplished by observing *I*(NF(a)) while turning the HCl flow on and off; see Figure 6. Quenching by F atoms is slower than by Cl atoms, and the data give $k_F^{NF} = (3 \pm 1) \times 10^{-13}$ cm^3 s^{-1}, which is consistent with the result in the literature[5], $(4 \pm 1) \times 10^{-13}$ cm^3 s^{-1}. Although the degree of quenching is small, the relative measurements should be reliable.

The Cl-atom quenching of NCl(a) was difficult to measure because precautions were necessary to avoid quenching of NCl(a) by F atoms. Also, the [NCl(a)] should be below 1×10^{12}

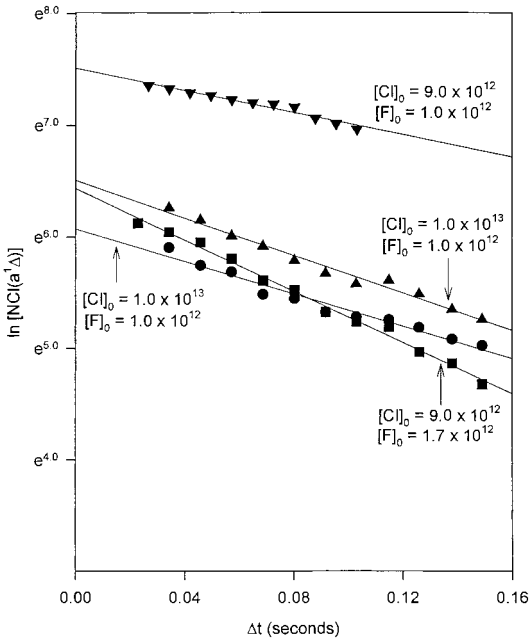

Figure 7. Pseudo-first-order NCl(a) decay plots for Cl-atom concentrations of approximately 1×10^{13} atoms cm^{-3}. The $[HN_3]_0$ was 2×10^{12} molecule cm^{-3} except for one experiment (□) for which it was 3.8×10^{12} molecule cm^{-3}. The F atoms were generated in the fore-reactor, Cl atoms were generated in the pre-reactor, and HN_3 was added at the reagent port.

molecule cm^{-3} to reduce the bimolecular self-destruction rate. To isolate the Cl-atom quenching reaction, NCl(a) was generated in the main reactor by adding a low concentration of HN_3 *at the reagent inlet* to F atoms that were generated by a discharge in CF_4 in the fore-reactor and Cl atoms generated in the F + HCl pre-reactor. The Cl-atom concentration was $\sim 1 \times 10^{13}$ atoms cm^{-3}, and the first-order decay of NCl(a) should be dominated by the k_{Cl}^{NCl}[Cl] term. The actual [Cl] and [F] present 0.04 s after the Cl/F + HN_3 flows have been mixed, which is the zero time for the quenching plots, were estimated by numerical integration of the rate equations for Cl and F with HCl and HN_3. Several semilog plots of I(NCl(a)) vs Δt are shown in Figure 7. Table 2 lists the initial $[Cl]_0$, $[F]_0$, and $[HN_3]_0$, and the slopes from plots of ln[NCl(a)] vs time and the contribution from k_F^{NCl}[F] for nine experiments. Since the [F] was not negligible in all experiments, adjustment for F-atom quenching must be considered. Experiment 6 was discarded because the F atom contribution to quenching is too large. The excess HN_3 in experiments 8 and 9 will give slow generation of NCl(a) from the Cl + HN_3 reaction; however, these k_{Cl}^{NCl} values seem as reliable as the others. The average of the eight experiments is $k_{Cl}^{NCl} = 1.1 \times 1.0^{-12}$ cm^3 s^{-1}. On the basis of these data, k_{Cl}^{NCl} was selected as $(1.0 + 1.0/-0.5) \times 10^{-12}$ cm^3 s^{-1}, which is about two times larger than k_{Cl}^{NF}.

III.B. The F/Cl/HN_3 Reaction System: Conversion of I(NX($a^1\Delta$)) to [NX($a^1\Delta$)]. The [NCl(a)] was estimated by comparing the NCl(a−X) emission intensity to the NF(a−X) intensity for a known [NF(a)] generated by the F + HN_3 system.[5] Although the HN_3 is nearly quantitatively converted to NF(a) + N_2, the observed yield is suppressed by the quenching reactions, and a kinetic model for the F/HN_3 system was developed to estimate the [NF(a)] for a given I(NF(a)). For simplicity, we used a branching fraction for NF(a) formation of unity from 2F + HN_3.

$$F + HN_3 \rightarrow HF + N_3 \quad (2a)$$

$$\rightarrow HNF + N_2 \quad (2b)$$

$$F + N_3 \rightarrow NF(a^1\Delta) + N_2 \quad (3)$$

$$F + NF(a^1\Delta) \rightarrow F + NF(X^3\Sigma^-) \quad (4)$$

$$NF(a^1\Delta) + NF(a^1\Delta) \rightarrow \text{products} \quad (5a)$$

$$\rightarrow NF(X^3\Sigma^-) + NF(b^1\Sigma^+) \quad (5b)$$

The quenching of NF(a) by HN_3 (2.1×10^{-13} cm^3 s^{-1})[5b] and NF(X) (3×10^{-13} cm^3 s^{-1})[6c] is not important for the conditions used here. Bimolecular self-quenching starts to become important for [NF(a)] > 5×10^{11} molecules cm^{-3} and $\Delta t \geq 0.05$ s. The rate constants for reactions 2−5 are summarized in Table 3.

The generation of NF(a) for two experiments is shown in Figure 8 together with the model calculations for [N_3] and [NF(a)]. All of the N_3 has reacted after 0.04 s and the [NF(a)] has reached its maximum value, which is 1.4 and 0.84×10^{12} molecules cm^{-3} for these two experiments according to the model. These data are consistent with nearly 100% conversion of HN_3 to NF(a), but with the [NF(a)] suppressed to 78 and 84% of the stoichiometric yield because of the bimolecular self-destruction process. In the next section, we will use the [NF(a)] predicted by the model from the initial $[HN_3]_0$ with excess $[F]_0$ and the observed NF(a−X) intensity to convert the NCl(a−X) emission intensities to absolute NCl(a) concentrations.

III.C. The F/Cl/HN_3 Reaction System: The Cl + N_3 Total Rate Constant and X_a. In order to describe the F/Cl/HN_3 system, the following reactions must be added to eqs 1−5 to complete the model.

$$Cl + HN_3 \rightarrow HCl + N_3 \quad (6a)$$

$$\rightarrow HNCl + N_2 \quad (6b)$$

$$Cl + NCl(a^1\Delta) \rightarrow Cl + NCl(X^3\Sigma^-) \quad (7)$$

$$F + NCl(a^1\Delta) \rightarrow F + NCl(X^3\Sigma^-) \text{ or } Cl + NF(X^3\Sigma^-) \quad (8)$$

$$2NCl(a^1\Delta) \rightarrow \text{products} \quad (9a)$$

$$\rightarrow NCl(X^3\Sigma^-) + NCl(b^1\Sigma^+) \quad (9b)$$

$$Cl + NF(a^1\Delta) \rightarrow Cl + NF(X^3\Sigma^-) \quad (10)$$

The NCl(a) + NF(a) reaction was not included in the model because no information is available for this reaction. The quenching of NCl(a) and NF(a) by NCl(X) and NF(X) have not been included because the rates are assumed to be less than the bimolecular self-destruction rates and because the ground-state NX concentrations are low. The Cl + HN_3 room temperature rate constant[12,13] is approximately 1.0×10^{-12} cm^3 s^{-1}. Unit branching to HCl + N_3 previously has been assumed, but a component giving HNCl + N_2 cannot be excluded.[9] The 300 K rate constants for the F/Cl/HN_3 reaction system are summarized in Table 3.

TABLE 2: Quenching of NCl($a^1\Delta$) by Cl Atoms

no.	$[Cl]_0$[a]	$[F]_0$[a]	$[HN_3]_0$[a]	total decay constant[b]	$k_F^{NCl}[F_t]$[c]	k_{Cl}^{NCl} [d]
1	1.2×10^{13}	1.6×10^{12}	1.0×10^{12}	24.9	14.8	9.2
2	1.0×10^{13}	1.0×10^{12}	2.0×10^{12}	7.18	0.20	8.2
3	9.0×10^{12}	1.7×10^{12}	2.0×10^{12}	11.6	1.70	13
4	1.2×10^{13}	2.6×10^{12}	2.0×10^{12}	24.4	11.7	13
5	1.1×10^{13}	1.9×10^{12}	2.0×10^{12}	15.9	3.4	13
6	8.2×10^{12}	3.8×10^{12}	2.0×10^{12}	33.2	31.2	3.0[e]
7	1.0×10^{13}	1.0×10^{12}	2.0×10^{12}	8.25	0.20	9.5
8	9.0×10^{12}	1.0×10^{12}	4.0×10^{12}	4.94	0.00	7.5
9	9.5×10^{12}	2.5×10^{12}	4.0×10^{12}	12.1	0.00	18
				selected value		10^{+10}_{-5}

[a] Concentrations are in atoms (molecules) cm^{-3}. [b] Total pseudo-first-order decay constant $= k_F^{NCl}[F_t] + k_{Cl}^{NCl}[Cl_t]$ from plots of I(NCl(a)) vs time. [c] Estimated from $[F_t]$ and $k_F^{NCl} = 2.2 \times 10^{-11}$ cm^3 $molecule^{-1}$ s^{-1}. [d] In 10^{-13} cm^3 $molecules^{-1}$ s^{-1} units. [e] Not included in the choice for the selected value, see text.

TABLE 3: The F/Cl/HN_3 Reaction System

	reaction	rate constant (cm^3 $molecules^{-1}$ s^{-1})	ref
1a	$Cl + N_3 \rightarrow NCl(a^1\Delta) + N_2$	$(1.5 \pm 0.6) \times 10^{-11}$	this work
1b	$Cl + N_3 \rightarrow NCl(b^1\Sigma^+) + N_2$	$\leq 1 \times 10^{-14}$	this work
1c	$Cl + N_3 \rightarrow NCI(X^3\Sigma^-) + N_3$	$\approx (1.5 \pm 0.6) \times 10^{-11}$	this work
2a	$F + HN_3 \rightarrow HF + N_3$	1.1×10^{-10}	5
2b	$F + HN_3 \rightarrow HNF + N_2$	$(6.3 \pm 1.8) \times 10^{-12}$	9
3a	$F + N_3 \rightarrow NF(a^1\Delta) + N_2$	$(5.0 \pm 2.0) \times 10^{-11}$	5b, 7
3b	$F + N_3 \rightarrow NF(b^1\Sigma^+) + N_2$	$(5.0 \pm 2.0) \times 10^{-13}$	5b
3c	$F + N_3 \rightarrow NF(X^3\Sigma^-) + N_3$	$< 7.5 \times 10^{-12}$	5b, 4c
4	$F + NF(a^1\Delta) \rightarrow F + NF(X^3\Sigma^-)$	$(4.0 \pm 2.0) \times 10^{-13}$	5b, 6c
5a	$NF(a^1\Delta) + NF(a^1\Delta) \rightarrow$ products[a]	$(5.0 \pm 2.0) \times 10^{-12}$	5b
5b	$NF(a^1\Delta) + NF(a^1\Delta) \rightarrow NF(b^1\Sigma^+) + NF(X^3\Sigma^-)$	$(6 \pm 1) \times 10^{-15}$	5b
6	$Cl + HN_3 \rightarrow HCl + N_3$	$(8.9 \pm 1.2) \times 10^{-13}$	12, 13
7	$Cl + NCl(a^1\Delta) \rightarrow Cl + NCl(a^1\Delta)$	$1.0^{+1.0}_{-0.5} \times 10^{-12}$	this work
8	$F + NCl(a^1\Delta) \rightarrow F + NCl(X^3\Sigma^-)$	$(2.2 \pm 0.7) \times 10^{-11}$	this work
9a	$NCl(a^1\Delta) + NCl(a^1\Delta) \rightarrow$ products[a]	$(7.2 \pm 0.9) \times 10^{-12}$	18[a]
9b	$NCl(a^1\Delta) + NCl(a^1\Delta) \rightarrow NCl(b^1\Sigma^+) + NCl(X^3\Sigma^-)$	$(1.5 \pm 0.4) \times 10^{-13}$	this work
10	$Cl + NF(a^1\Delta) \rightarrow Cl + NF(X^3\Sigma^-)$	$(6 \pm 2) \times 10^{-13}$	this work

[a] All bimolecular self-destruction rates are defined as $d[NX]/dt = k[NX]^2$.

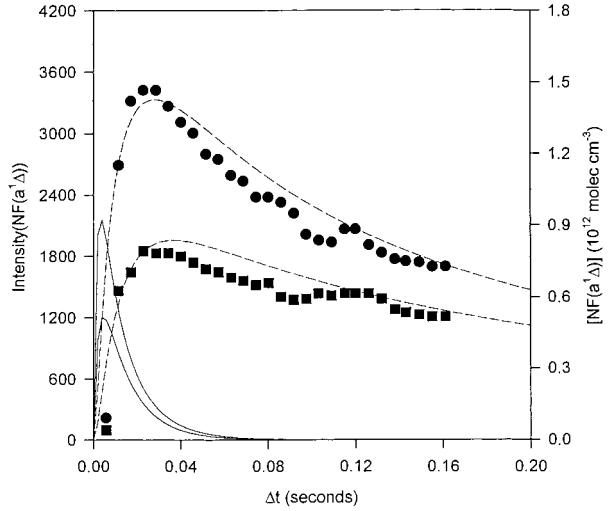

Figure 8. Calibration of the I(NF(a) vs the NF($a^1\Delta$) concentration. The emission intensity is matched with the [NF(a)] predicted from the $F + HN_3$ kinetic model. The experimental conditions are ●, $[F] = 5.0 \times 10^{12}$ and $[HN_3] = 2.0 \times 10^{12}$; ■, $[F] = 3.5 \times 10^{12}$, and $[HN_3]_0 = 1.0 \times 10^{12}$ cm^{-3} at the reagent inlet. The maxima correspond to [NF(a)] = 1.4 and 0.84×10^{12} molecules cm^{-3}, or 78% and 84% of the initial $[HN_3]$, respectively. The solid curves show the calculated $[N_3]$; NF($a^1\Delta$) formation is essentially complete after 0.04 s.

The total $Cl + N_3$ rate constant and X_a were evaluated by experiments described below. In these experiments for which Cl and F atoms compete for N_3, a $[HN_3]_0$ of 2×10^{12} molecules cm^{-3} was added at the reagent inlet to [F] and [Cl] that had been generated in the fore- and pre-reactors, respectively. Typically, $[HCl]_0 = 1.0 \times 10^{13}$ and $[F]_0 = 8.0 \times 10^{12}$ in the pre-reactor with $[F]_0 \cong 5.0 \times 10^{12}$ cm^{-3} in the fore-reactor. The slight excess of HCl continues to react with F atoms in the outer reactor until $[HN_3]$ is added at the reagent inlet. The resulting [F] and [Cl] at the reagent inlet are $[Cl] = (0.8-1.0) \times 10^{13}$ and $[F] \cong 3.0 \times 10^{12}$ cm^{-3}. The excess [F], relative to $[HN_3]_0$, was kept low to minimize quenching of NCl(a); the actual [F] was measured by observing I(HF) with added HCl, after the I(HF) was calibrated for known [F] by titration.

The yield of NF(a) is controlled by the relative magnitudes of the k_1[Cl] vs k_3[F] terms, and k_1 can be estimated from the reduction in the yield of NF(a) as a function of Cl-atom concentration. The peak [NF(a)], for excess [F] but with [Cl] = 0, and the decay rate of NF(a) shown in the top panel of Figure 9 is accurately predicted by the model (and also for the data shown in Figure 8). The addition of [Cl] reduces the [NF(a)] and also reduces its decay rate, because the main NF(a) decay process is bimolecular self-destruction. The top panel also shows the NF(a) and NCl(a) concentrations for $[F]_0 \approx {}^1/_2$-$[HN_3]_0$ and [Cl] > [F]. The presence of some NF(a) suggests that k_1 and k_3 must be of comparable magnitude. The time dependence of [NF(a)] for an experiment with $[HN_3]_0 = 4.0 \times 10^{12}$ and the [F] and [Cl] given in the caption is shown in the lower panel of Figure 9 together with predictions from the model for $k_1 = 20$, 3, and 1×10^{-11} cm^3 s^{-1}. The experimental NF(a) concentration agrees best with the model for $k_1 = 3 \times 10^{-11}$ cm^3 s^{-1}; a value for k_1 as large as 2×10^{-10} cm^3 s^{-1} clearly is unacceptable. Two more experiments with the growth of [NF-

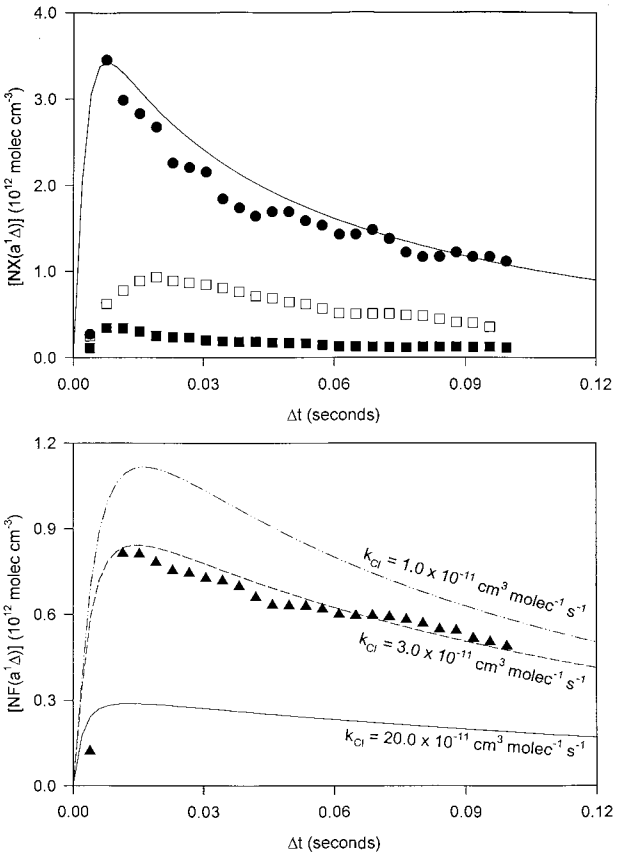

Figure 9. NF(a) concentration vs time in the F/Cl/HN_3 reaction system. The [F] was produced in the fore-reactor by a microwave discharge in CF_4, and [Cl] was generated using the F + HCl reaction in the pre-reactor. Hydrogen azide was added at the reagent inlet. The experimental conditions for the upper panel are ●, $[HN_3] = 4.0 \times 10^{12}$, [F] $= 16 \times 10^{12}$ molecules cm^{-3} with [Cl] equal zero; the solid line is the model calculation. The second data set in the upper panel shows the NF(a) (■) and NCl(a) (□) concentration for ($[HN_3] = 4.0 \times 10^{12}$, [Cl] $= 9.0 \times 10^{12}$, and [F] $= 2.5 \times 10^{12}$ molecule cm^{-3} at the reagent inlet. The lower panel shows the NF(a) concentration for $[HN_3]_0 = 4.0 \times 10^{12}$, [Cl] $= 9.5 \times 10^{12}$, and [F] $= 5.1 \times 10^{12}$ cm^{-3} together with model predictions (dashed curves) for [NF(a)] for $k_1 = 1$, 3, and 20×10^{-11} cm^3 $molecules^{-1}$ s^{-1}.

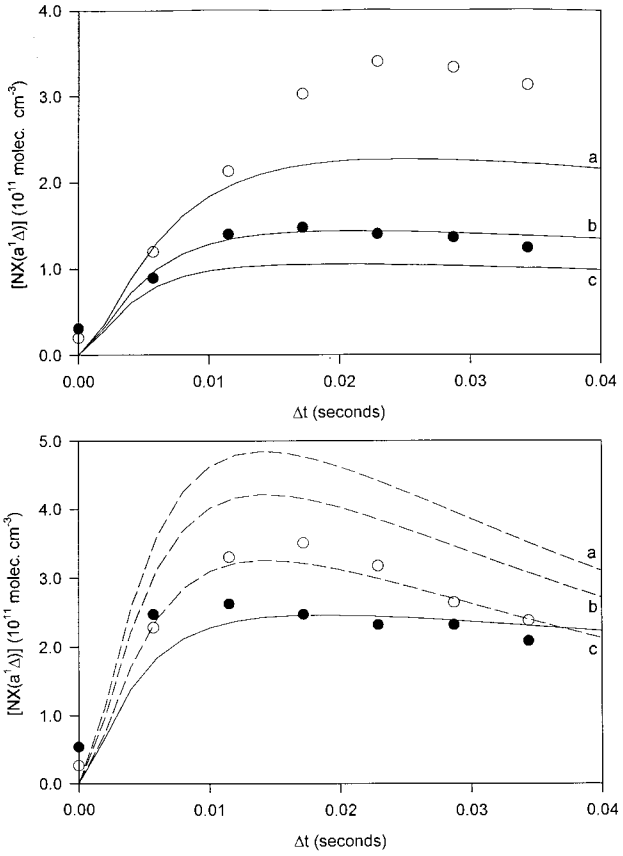

Figure 10. Plots of NF(a) and NCl(a) concentrations for short time. The observed [NF(a)] and [NCl(a)] are shown by the ● and ○ symbols, respectively, and the model predictions for [NF(a)] and [NCl(a)] are given by the solid and broken lines, respectively. The experimental conditions for the upper panel were [F] $= 1.7 \times 10^{12}$, [Cl] $= 9.0 \times 10^{12}$, $[HN_3]_0 = 2.0 \times 10^{12}$ molecules cm^{-3} and for the lower panel [F] $= 2.6 \times 10^{12}$, [Cl] $= 1.2 \times 10^{13}$, $[HN_3]_0 = 2.0 \times 10^{12}$ molecules cm^{-3}. In the upper panel, the model results for [NF(a)] with $k_1 = 1$ (a), 3 (b), and 5 (c) $\times 10^{-11}$ cm^3 $molecules^{-1}$ s^{-1} are shown. In the lower panel, k_1 was fixed at 3.0×10^{-11} cm^3 $molecules^{-1}$ s^{-1} (note that the solid line fits the NF(a) data), and X_a was varied from 0.50 (a), 0.43 (b), and 0.37 (c), respectively, for comparison with the [NCl(a)].

(a)] at early time better resolved are shown in Figure 10; the [NF(a)] for these experiments also are adequately represented by $k_1 = 3 \times 10^{-11}$ cm^3 s^{-1}.

In principle, the magnitude of k_1 can also be obtained from the rate of NF($a^1\Delta$) and NCl($a^1\Delta$) growth at early times, which is determined by the sum of $k_1 + k_3$. For small $[HN_3]$ and large [F] and [Cl], the formation of NF($a^1\Delta$) and NCl($a^1\Delta$) is described by consecutive first-order reaction kinetics with N_3 as the intermediate. The rise time for the [NF(a)] and [NCl(a)] corresponds to the decay time of N_3. The growth of NF(a) or NCl(a) shown in Figure 10 is consistent with $k_1 = (2-4) \times 10^{-11}$ cm^3 s^{-1}; it is not compatible with a value $> 5 \times 10^{-11}$ cm^3 s^{-1}. The data in Figures 9 and 10 indicate that k_1 must be somewhat smaller than k_3 and we favor a value of $(3 \pm 1) \times 10^{-11}$ cm^3 $molecules^{-1}$ s^{-1}. These results depend on the reduction in [NF(a)] for known [Cl] and [F] and not upon $\tau_{NCl(a)}$. An explicit check on the possible interference of HF(3−0) emission with the NF(a−X) intensity was made, and for the conditions used to obtain the data of Figures 9 and 10 the HF(3−0) emission was not important.

The actual yield of NCl(a) depends on $X_a \cdot k_1$, and the ratio of [NCl(a)] to [NF(a)] was examined to obtain an estimate for X_a. The F atoms, $(1-2) \times 10^{12}$ atoms cm^{-3}, were generated in the fore-reactor, and large [Cl] (typically 1×10^{13} atoms cm^{-3}) were produced in the F + HCl pre-reactor to obtain the highest yields of NCl(a). The [NCl(a)] were obtained by comparing the NCl(a−X) and NF(a−X) relative intensities with adjustment for radiative lifetimes and spectral response for a known [NF(a)]. The [NF(a)] calibration is based on the model calculation for a given $[HN_3]_0$ with excess $[F]_0$ and [Cl] = 0; see Figure 8. Some [NCl(a)] data were already shown in Figures 9 and 10. However, the most pertinent results for determination of X_a are in Figure 11. The data are first examined by inspecting the [NF(a)] and [NCl(a)] on the same plot; see the inserts in Figure 11. The solid line at the top of the figures indicates the *minimum* expected yield for NF(a) + NCl(a) For $X_a = 1.0$; this expected yield was estimated as $0.5[F]_0$ because $[Cl]_0 \gg [HN_3]_0 > [F]_0$ and nearly all of the F atoms should go toward production of N_3. The actual observed yield of NF(a) + NCl(a), even with accounting for quenching, should be higher than $0.5[F]_0$, if $X_a = 1.0$. The data in Figure 11 are below the expected limit, and X_a must be ≤ 1.0 (for our choice of $\tau_{NCl(a)}$) because the branching fraction for NF(a) is known to be very close to unity.

The NCl(a) concentration for the whole time regime is also shown in Figure 11. Comparison with the model calculation shows that the experimental data are best fit by $k_{1a} = 1.3 \times 10^{-11}$ cm^3 s^{-1}, which corresponds to $X_a = 0.43$. The high [Cl]

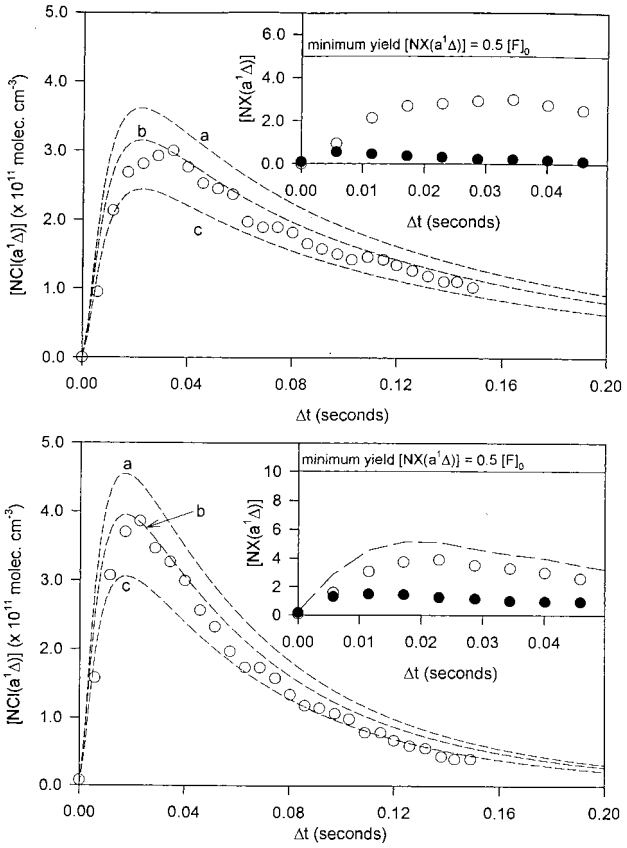

Figure 11. Generation of $NCl(a^1\Delta)$ in the F/Cl/HN_3 system. The starting concentrations for the upper and lower panels are [F] = 1.0×10^{12}, [Cl] = 1.0×10^{13}, $[HN_3]_0 = 2.0 \times 10^{12}$ cm^{-3} and [F] = 1.9×10^{12}, [Cl] = 1.1×10^{13}, $[HN_3]_0 = 2.0 \times 10^{12}$ cm^3, respectively. The total Cl + N_3 rate constant was fixed at 3.0×10^{-11} cm^3 s^{-1}, and calculations a−c represent the model prediction for X_a = 0.5, 0.43, and 0.33, respectively. The decay of [NCl(a)] is mainly from quenching by Cl atoms. The inset plots compare the observed [NF(a)] and [NCl(a)] with the theoretical minimum yield of [NX(a)] (solid line); the broken line in the lower plot indicates the sum of [NF(a)] and [NCl(a)].

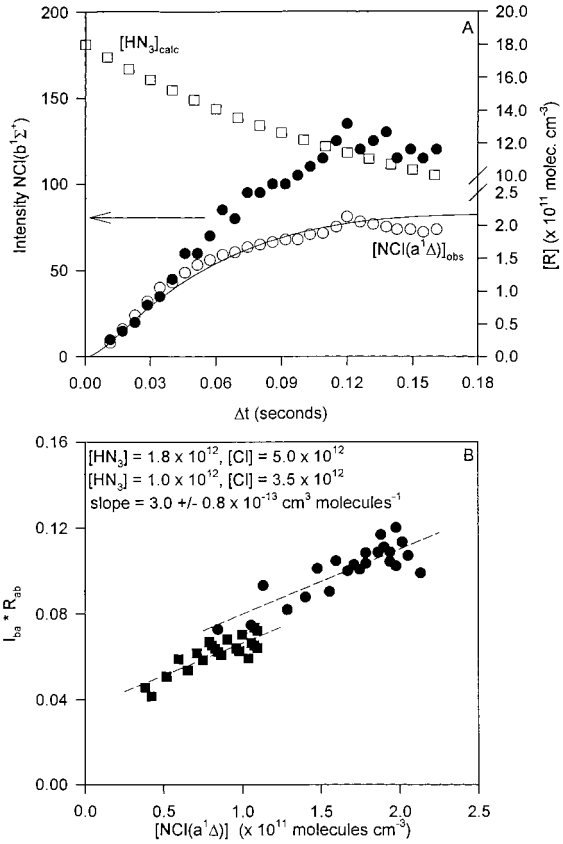

Figure 12. (A) Dependence of the NCl(b−X) emission intensity on reaction time in the Cl + HN_3 reaction. The experimental [NCl(a)] points and the results from model calculations are shown for comparison. The $[HN_3]$ points are calculated for the initial concentrations of $[HN_3] = 1.8 \times 10^{12}$ and [Cl] = 5×10^{12} molecules cm^{-3}. (b) Plot of I_b/I_a vs [NCl(a)]. The energy-pooling rate constant was obtained from the slope of the line; see text. R_{ab} is the ratio of response of the detector at 1077 vs 665 nm.

chosen in order to convert as much of the $[N_3]$ to NCl(a) as possible results in the decay of NCl(a) because of quenching by Cl atoms. Thus, the selection of k_{1a} is somewhat dependent on the reliability of k_{Cl}^{NCl} and the other quenching rates of NCl(a). However, the model does fit the decay rate of [NCl(a)], which suggest that quenching has been treated satisfactorily and gives confidence in the assignment of X_a. The most important factor for X_a is the value chosen for the radiative lifetime; if a longer $\tau_{NCl(a)}$ is more appropriate then [NCl(a)] and X_a will increase, vide infra.

III.D. Generation Processes for NCl($b^1\Sigma^+$). The NCl(b−X) emission at 665 nm is observed throughout the reactor, although the emission is most intense at the front of the reactor where the F + HN_3 reaction occurs. At least, three processes could give NCl(b): (i) direct formation from the Cl + N_3 reaction, (ii) energy pooling from interaction of two NCl(a) molecules, and (iii) vibrational-to-electronic energy transfer between HF($v \geq 2$) and NCl(a).

The energy-pooling process is best studied in the Cl + HN_3 reaction system, because HF(v) molecules are absent. The radiative lifetime for NCl(b) is 2.0 + 0.4 ms[24], and a steady-state analysis can be used for the kinetics because the loss rate due to radiation is greater than the generation rate. Direct formation from reaction 1b and formation from energy pooling can be distinguished by observing [NCl(b)] vs time. Since the Cl + HN_3 rate is much slower than the Cl + N_3 rate, the steady-state condition can be applied to $[N_3]$ and to [NCl(b)]. The combined rate law for NCl(b) formation in the Cl + HN_3 system is given below.

$$[\mathrm{NCl(b)}] = \frac{k_{1b}[N_3][\mathrm{Cl}] + k_{9b}[\mathrm{NCl(a)}]^2}{\tau_b^{-1}}$$

$$= \frac{(k_6[HN_3]/k_1)k_{1b}[\mathrm{Cl}] + k_{9b}[\mathrm{NCl(a)}]^2}{\tau_b^{-1}} \qquad (11)$$

If reaction 1b is dominant, the [NCl(b)] will follow $[HN_3]$ and the I(b) will be largest at early time. On the other hand, if energy pooling is the dominant mechanism, the [NCl(b)] will follow $[NCl(a)]^2$ and grow with time. The time dependence of the experimentally observed I(NCl(b)) is shown in Figure 12a. The [NCl(b)] does grow with [NCl(a)], and energy-pooling is the dominant formation process in the Cl + HN_3 system. The energy-pooling rate constant can be obtained using the steady-state expression above. Rearranging the equation and replacing the concentration ratio by the intensity ratio gives eq 12.

$$I_b/I_a = k_{9b}[\mathrm{NCl(a)}]/\tau_a^{-1} \qquad (12)$$

This expression is independent of reaction time (after the induction time), and a plot of I_b/I_a vs [NCl(a)] should give k_{9b}.

The plots in Figure 12b, which were constructed using the NF(a) from a known $[HN_3]_0$ with excess [F] to calibrate for [NCl(a)], give $k_{9b} = (1.5 \pm 0.4) \times 10^{-13}$ cm^3 s^{-1}. The total bimolecular quenching rate constant[18b] has been reported as $(7.2 \pm 0.9) \times 10^{-12}$ cm^3 s^{-1}, so the branching fraction for NCl(b) formation in reaction 9 is ~0.02. Exton, Gilbert, and Coombe[25] also observed NCl(b) at $\Delta t > 2$ ms in the H + NCl_3 reaction system. They attributed the formation of NCl(b) to the H + NCl_2 reaction. With benefit of hindsight, the energy-pooling process would be more consistent with their observed time profile for [NCl(b)], which seems to follow [NCl(a)].

Calculations were done to set an upper limit to X_b from the data in Figure 12. From the assigned value for k_{9b} and [NCl(a)], the [NCl(b)] from eq 9b could be evaluated. An additional contribution of 20% from the direct reaction to [NCl(b)] could have been detected at early time; this limit to NCl(b) from eq 1b leads to $X_b \leq 0.01$. In the absence of F atoms, the main mechanism for NCl(b) generation is the NCl(a) + NCl(a) energy-pooling reaction.

The energy exchange process between HF($v \geq 2$) and NCl(a) was identified by adding H_2S to the reactor at the last inlet, which is normally used for ethane, to a flow containing NF(a) and NCl(a) generated in the F/Cl/HN_3 reaction system with excess F atoms. The addition of H_2S creates vibrationally excited HF($v \leq 4$), and strongly enhanced NF(b) and NCl(b) emission intensities were observed at the H_2S inlet. This confirms that the NCl(b−X) emission observed in the F/Cl/HN_3 primary interaction zone mainly arises from the vibrationally excited HF($P_1 - P_4 = 36{:}36{:}22{:}06$)[5a] produced from F + HN_3. Although we were able to identify the V → E transfer mechanism, these experiments were not suitable for determining the rate constant.

The branching fraction for NCl(a) formation in reaction 1 also was qualitatively examined in the Cl + HN_3 system.[23a] A flow of [Cl] was generated from the F + HCl pre-reactor and added to the HN_3 flow. The experimental [NCl(a)] was calibrated from observation of the [NF(a)] generated from the same $[HN_3]$ in excess [F] on the same day. Figure 12 shows the [NCl($a^1\Delta$)] observed for one set of conditions. Model results, including all known NCl(a) quenching processes, are shown for comparison. The data are consistent with line b, $k_{1a} = 1.5 \times 10^{-11}$ cm^3 s^{-1} or $X_a = 0.5$. Although the X_a value is very sensitive to the rate constants used for reactions 6 and 7 and the assumption that reaction 6b is not important, the Cl + HN_3 results are consistent with the conclusions from the mixed F/Cl/HN_3 system.

IV. Discussion

The experiments reported here indicate that reaction 1 is very similar to reaction 3 in terms of both product branching fractions and total rate constant. Our data, similar data from Henshaw et al.,[18a] and laser-induced fluorescence experiments[9] that monitored $[N_3]$ decay vs [Cl] all favor a k_1 value of in the range $(3 \pm 1) \times 10^{-11}$ cm^3 s^{-1}. Jourdain and co-workers[26] assigned a k_1 value of $(0.75-1.5) \times 10^{-11}$ cm^3 s^{-1} based on modeling the Cl + ClN_3 reaction system. The $(3 \pm 1) \times 10^{-11}$ cm^3 s^{-1} value is an order of magnitude smaller than an early report,[7] which also was based upon the reduction in [NF(a)] when Cl atoms were generated in the flow reactor. In that work, Cl atoms were generated in the reactor by the F + Cl_2 reaction for a starting F-atom concentration of 1×10^{14} atom cm^3. The F + Cl_2 reaction was used both to titrate the [F] and to generate a known [Cl]. The authors noted that the NF(a) concentration decayed along the reactor ("a period of many milliseconds"), and an extrapolation to zero decay time was made to estimate the NF(a) intensity that should be associated with the NF(a) formed from F + N_3 in competition with Cl + N_3. Without knowing the extent of the decay of NF(a) in the presence of the added Cl_2, reanalysis of these experiments is not possible. Although the discrepancy has not been resolved,[27] the weight of evidence now favors $k_3 \lesssim k_1$. The Liu et al.[7] paper, which mainly reported a direct measurement of the rate constant for the F + N_3 reaction, was part of the important effort by the Denver laboratory to develop the NCl(a) molecule as an energy storage system.[28]

Selection of the best X_a value depends on $\tau_{NCl(a)}$. Our assignment of $X_a \approx 0.43$ is based on $\tau_{NCl(a)} = 2$ s. If the true lifetime is closer to the matrix-based lifetime[21] of 3.7 s, the X_a from out data would increase to nearly ~0.8. If the calculated lifetime of 2.4 s is used, our data give $X_a \geq 0.5$. Work in the Denver laboratory[27] and the thermal dissociation experiments using infrared laser sensitization with SF_6/ClN_3 mixtures[29] also have favored an X_a value ≳0.5. However, X_a is dependent on the choice for $\tau_{NCl(a)}$ for each of these experiments. Obtaining a more reliable X_a will require an absolute NCl(a) concentration measurement that does not depend on the NCl(a−X) emission intensity, or experiments with simultaneous measurement of the relative NCl(X) and NCl(a) concentrations at early times in the Cl + N_3 reaction. The present experiments have demonstrated that X_a is probably larger than 0.5, and that NCl(b) formation is negligible, but the question of how much ground-state NCl(X) is formed in reaction 1 needs more study.

The X + N_3 reactions can be discussed in terms of the unimolecular reactions of the chemically activated $XN_3(\tilde{X})$ molecules. The dissociation pathways for FN_3 and ClN_3 can be compared to HN_3 with adjustments for different thermochemistry and expected locations of the crossing of the potential energy surfaces. Dissociation on the $HN_3(\tilde{X}^1A')$ potential energy surface correlates to HN($a^1\Delta$) + N_2; however, a crossing with the triplet potential, $\tilde{a}^3A''$, occurs in the 35 kcal mol^{-1} range before the singlet surface reaches its dissociation barrier of ~49 kcal mol^{-1}.[30] The interaction between the singlet and triplet potentials is sufficiently strong that thermal and infrared laser initiated dissociation[30,31] gives mainly NH($X^3\Sigma^-$), as does dissociation of chemically activated HN_3 formed by H + N_3.[32] The existence of a potential barrier along the singlet exit channel for dissociation has been inferred from the small quenching rate[33] of NH(a) by N_2 and by the translational energy found for NH($a^1\Delta$) following infrared, multiphoton, laser-driven dissociation of HN_3.[31]

The high efficiency for NF(a) formation both from thermal dissociation[34] and from chemical activation[5] by F + N_3 is explained by the weak FN−N_2 bond, which results in the crossing of the singlet and triplet FN-N_2 potentials near the dissociation limit of the singlet potential. In fact, calculations suggest that the crossing position may be even at longer range than the barrier for dissociation.[34] However, the quenching rate of NF(a) by N_2 is very slow[5] at 300 K, and the singlet−triplet potential surface intersection is not accessible to room temperature collisions.

The ClN_3 dissociation enthalpy[35,17] giving NCl(a) + N_2 can be estimated as ~11 kcal mol^{-1}, whereas that for NCl(X) + N_2 is −16 kcal mol^{-1}. The branching fraction for NCl(a) formation from Cl + N_3 (the vibrational energy of ClN_3 is about 58 kcal mol^{-1}) and by multiphoton infrared laser sensitization of SF_6/ClN_3 mixtures are both significant, and they may even approach unity. The quenching of NCl(a) by N_2 has a small rate constant.[23] The available evidence certainly shows that the

crossing of the potentials for the ClN_3 system resembles FN_3 more than HN_3. If X_a is less than unity, the explanation presumably is that the singlet−triplet potential surface crossing is close to, but below, the dissociation barrier on the singlet surface.[29]

The rate constants for F and Cl atoms with NF(a) are $\approx 0.5 \times 10^{-12}$ cm^3 s^{-1} at 300 K, and the quenching rates are slow at modest concentrations of F or Cl atoms. Quenching of NCl(a) by Cl atoms is about two times faster than for NF(a), but the rate still is not too serious. However, quenching of NCl(a) by F atoms has a sizeable rate constant, 2.2×10^{-11} cm^3 s^{-1}, and the F atom concentration must be carefully controlled. Since both NF(a) + Cl and NCl(a) + F correlate to excited states of the NFCl radical with similar energies, the difference in quenching rates could be associated with potential surface crossings for excited states correlating to NCl(X) + F and/or NF(X) + Cl. Another possibility could be a larger activation energy barrier in the approach of Cl atoms to NF(a) than for the approach of F atoms to NCl(a). More information about the excited states of the NFCl radical would be useful.

IV. Conclusions

The Cl + N_3 reaction has been shown to be similar to the F + N_3 reaction; these gas-phase reactions are useful chemical sources of NCl($a^1\Delta$) and NF($a^1\Delta$) molecules, respectively. Both reactions proceed by recombination followed by unimolecular decomposition on the ground singlet-state potential. The 300 K rate constants for Cl + N_3 is $(3 \pm 1) \times 10^{-11}$ cm^3 s^{-1}, and the branching fraction for NCl($a^1\Delta$) formation is $\gtrsim 0.43$ for an assumed radiative lifetime of NCl($a^1\Delta$) of 2 s. If the true lifetime is longer, the branching fraction will be increased. Direct formation of NCl($b^1\Sigma^+$) from the Cl + N_3 reaction is a minor component. The more important pathways for NCl($b^1\Sigma^+$) formation in the F/Cl/HN_3 reaction system is by V−E transfer between HF($v \geq 2$) and NCl($a^1\Delta$) and by bimolecular energy pooling between NCl($a^1\Delta$) molecules. A systematic investigation of the H + NCl_2 reaction system[25] with determination of the NCl($a^1\Delta$) product branching fractions for comparison with the H + NF_2 reaction would be instructive.

The NCl($a^1\Delta$) molecule also is like NF($a^1\Delta$) in that the quenching rate by the parent halogen atom is not very important, $k_{Cl}^{NCl} \cong (1.0 + 1.0/-0.5) \times 10^{-12}$ cm^3 s^{-1}. However, NCl(a) is quenched by F atoms with a 300 K rate constants of $(2.2 \pm 0.7) \times 10^{-11}$ cm^3 s^{-1}, and the F atom concentration must be controlled to maintain a stable concentration of NCl($a^1\Delta$) in the F/Cl/HN_3 reaction system. The products from F + NCl($a^1\Delta$) could be either NF(X) or NCl(X), but indirect arguments favor NCl(X). The rate constant for quenching of NF($a^1\Delta$) by Cl atoms was measured to be $(6 \pm 2) \times 10^{-13}$ cm^3 s^{-1}, which is slightly larger than for F atoms ($(4 \pm 1) \times 10^{-13}$ cm^3 s^{-1}).

Acknowledgment. This work was supported by the U.S. Air Force under Grant F49620-96-1-0110 from the Air Force Office of Scientific Research. We thank Dr. Kevin Hewett of Kansas State University for preparation of Figure 2. We also acknowledge extensive discussions with Professor R. Coombe and Dr. T. Henshaw about the chemistry of NCl($a^1\Delta$).

References and Notes

(1) (a) Clyne, M. A. A.; White, I. F. *Chem. Phys. Lett.* **1970**, *6*, 465. (b) Cheah, C. T.; Clyne, M. A. A.; Whitefield, P. D. *J. Chem. Soc., Faraday Trans. 2*, **1980**, *76*, 711.

(2) (a) Herbelin, J. M.; Cohen, N. *Chem. Phys. Lett.* **1973**, *20*, 605. (b) Herbelin, J. M. *Chem. Phys. Lett.* **1976**, *42*, 367.

(3) Malins, R. J.; Setser, D. W. *J. Phys. Chem.* **1981**, *85*, 1342.

(4) (a) Koffend, J. B.; Weiller, B. H.; Heidner, R.F., III. *J. Phys. Chem.* **1992**, *96*, 9315. (b) Heidner, R. F., III, Helvajian, H.; Holloway, J. S.; Koffend, J. B. *J. Phys. Chem.* **1989**, *93*, 7818. (c) Bradburn, G. R.; Lilenfeld, H. V. *J. Phys. Chem.* **1991**, *95*, 555.

(5) (a) Habdas, J.; Wategaonkar, S.; Setser, D. W. *J. Phys. Chem.* **1987**, *91*, 451. (b) Du, K. Y.; Setser, D. W. *J. Phys. Chem.* **1990**, *94*, 2425.

(6) (a) Du, K. Y.; Setser, D. W. *J. Phys. Chem.* **1992**, *96*, 2553. (b)-Wategaonkar, S.; Du, K. Y.; Setser, D.W. *Chem. Phys. Lett.* **1992**, *189*, 586. (c) Du, K. Y.; Setser, D. W. *J. Phys. Chem.* **1993**, *97*, 5266.

(7) Liu, X.; MacDonald, A.; Coombe, R. D. *J. Phys. Chem.* **1992**, *96*, 4907.

(8) (a) David, S.J.; Coombe, R.D. *J. Phys. Chem.* **1985**, *89*, 5206. (b) Ongstad, A. P.; Henshaw, T. L.; Lawconnel, R. I.; Thorpe, W. G. *J. Phys. Chem.* **1990**, *94*, 6724.

(9) Hewett, K.; Setser, D. W. *J. Phys. Chem.* **1997**, *101*, 9125.

(10) Chen, J.; Dagdigian, P. J. *J. Chem. Phys.* **1992**, *96*, 7333; **1993**, *98*, 3554.

(11) (a) Davis, S. J.; Rawlins, W. G.; Piper, L. G. *J. Phys. Chem.* **1989**, *93*, 1078. (b) Davis, S. J.; Piper, L. G. *J. Phys. Chem.* **1990**, *94*, 4525.

(12) Yamasaki, K.; Fueno, T.; Kajimoto, O. *Chem. Phys. Lett.* **1983**, *94*, 425.

(13) Manke, G., II; Setser, D. W. *J. Phys. Chem.* **1998** *102*, 153.

(14) (a) Coombe, R. D.; Pritt, A. T., Jr.; *Chem. Phys. Lett.* **1978**, *58*, 606. (b)Pritt, A. T., Jr., Patel, D.; Coombe, R. D. *J. Mol. Spectrosc.* **1981**, *87*, 401. (c) Pritt, A. T., Jr.; Patel, D.; Coombe, R. D. *Int. J. Chem. Kinet.* **1984**, *16*, 977.

(15) Clyne, M.A.A.; MacRobert A.; *J. Chem. Soc., Faraday Trans. 2* **1983**, *79*, 283; **1985**, *81*, 159.

(16) (a) Martin, J. L. M.; Francois, J. P.; Gijbels, R. *J. Chem. Phys.* **1990**, *93*, 4485. Continetti, R. E.; Cyr, D. R.; Osborn, D. L.; Leahy, D. J.; Neumark, D. M. *J. Chem. Phys.* **1993**, *99*, 2616.

(17) Xantheas, S. S.; Dunning, T. H., Jr.; Mavridis, A. *J. Chem. Phys.* **1997**, *106*, 3280.

(18) (a) Henshaw, Y. L.; Herrerra, S. D.; Schlie, L. A. *J. Phys. Chem. A* **1998**, *102*, 6239. (b) Henshaw, T. L.; Herrera, S. D.; Haggquist, G. W.; Schlie, L. A. *J. Phys. Chem. A*, **1997**, *101*, 4048. (c) Ray, A. J.; Coombe, R. D. *J. Phys. Chem.* **1994**, *98*, 8940.

(19) Hewett, K.; Setser, D. W. *J. Phys. Chem.* **1998**, *102*, 6274.

(20) Yarkony, D. R. *J. Chem. Phys.* **1987**, *86*, 1642.

(21) Becker, A. C.; Schurath, U. *Chem. Phys. Lett.* **1989**, *160*, 586.

(22) Werzberg, E.; Grimley, A. J.; Houston, P. L., *Chem. Phys. Lett.* **1978**, *57*, 373.

(23) (a) Manke, G., II; Hewett, K.; Setser, D. W. *J. Phys. Chem. A*, To be submitted. (b) Manke, G., II. Ph.D. Thesis, Kansas State University, 1998.

(24) Zhao, Y.; Setser, D. W. *J. Chem. Soc., Faraday Trans.* **1995**, *91*, 2979.

(25) Exton, D. B.; Gilbert, J. V.; Coombe, R. D. *J. Phys. Chem.* **1991**, *95*, 2692.

(26) Jourdain, J. L.; LeBras, G.; Poulet, G. Combourieru, *J. Combust. Flame 34*, 13.

(27) Coombe, R. D. 1998, private communications.

(28) Ray, A. J.; Coombe, R. D. *J. Phys. Chem.* **1995**, *99*, 7849. See also several other papers in the series.

(29) Benard, D. J.; Chowdhury, M. A.; Winker, B. K.; Seder, T. A.; Michels, H. H. *J. Phys. Chem.* **1990**, *94*, 7507.

(30) (a) Alexander, M. H.; Werner, H-J.; Hemmer, T.; Knowles, P. J. *J. Chem. Phys.* **1990**, *93*, 3307. (b) Alexander, M. H.; Wesner, H-J.; Dagdigian, P. J. *J. Chem. Phys.* **1988**, *89*, 1388.

(31) (a) Foy, B. R.; Casassa, M. P.; Stephenson, J. C.; King, D. S. *J. Chem. Phys.* **1988**, 89, 608; **1990**, *92*, 2782; **1989**, *90*, 7037. (b) Stephenson, J. C.; Casasa, M. P.; King, D. S. *J. Chem. Phys.* **1988**, *89*, 1378.

(32) Chen, J.; Quinones, E.; Dagdigian, P. J. *J. Chem. Phys.* **1989**, *90*, 7603; **1990**, *93*, 4033.

(33) (a) Freitag, F.; Rohrer, F.; Stuhl, F. *J. Phys. Chem.* **1989**, *93*, 3170. (b)Hack, W.; Wilms, A. *J. Phys. Chem.* **1989**, *93*, 3540. (c) Hack, W.; Rathmanu, K. *J. Phys. Chem.* **1992**, *96*, 47. (d) Nelson, H. H.; McDonald, J. R.; Alexander, M. H. *J. Phys. Chem.* **1990**, *94*, 3291.

(34) Benard, D. J.; Winker, B. K.; Seder, T. A.; Cohn, R. H. *J. Phys. Chem.* **1989**, *93*, 4790.

(35) Paillard, C.; Moreau, R.; Combourieu, J. *Compt. Rend.* **1967**, *264*, 832.